Chemistry & Biology
Article

Mutational Analysis of the Quorum-Sensing Receptor LasR Reveals Interactions that Govern Activation and Inhibition by Nonlactone Ligands

Joseph P. Gerdt,[1,3] Christine E. McInnis,[1,3] Trevor L. Schell,[1] Francis M. Rossi,[2] and Helen E. Blackwell[1,*]
[1]Department of Chemistry, University of Wisconsin–Madison, Madison, WI 53706, USA
[2]Department of Chemistry, SUNY Cortland, Cortland, NY 13045, USA
[3]Co-first author
*Correspondence: blackwell@chem.wisc.edu
http://dx.doi.org/10.1016/j.chembiol.2014.08.008

SUMMARY

Gram-negative bacteria use *N*-acyl L-homoserine lactone (AHL) quorum-sensing (QS) signals to regulate the expression of myriad phenotypes. Non-native AHL analogs can strongly attenuate QS receptor activity and thereby QS signaling; however, we currently lack a molecular understanding of the mechanisms by which most of these compounds elicit their agonistic or antagonistic profiles. In this study, we investigated the origins of striking activity profile switches (i.e., receptor activator to inhibitor, and vice versa) observed upon alteration of the lactone head group in certain AHL analogs. Reporter gene assays of mutant versions of the *Pseudomonas aeruginosa* QS receptor LasR revealed that interactions between the ligands and Trp60, Tyr56, and Ser129 govern whether these ligands behave as LasR activators or inhibitors. Using this knowledge, we propose a model for the modulation of LasR by AHL analogs—encompassing a subtly different interaction with the binding pocket to a global change in LasR conformation.

INTRODUCTION

Although bacteria were once considered simple organisms that functioned as single cells, we now know that they often live as multicellular societies cooperating and competing with each other to exploit the resources in their surroundings (Schuster et al., 2013). Any society needs communication among its members, and bacteria use quorum sensing (QS) as a mechanism to sense their local population densities. When a "quorum" of bacteria is reached, the microbes alter their behavior to a phenotype that is more appropriate for a dense, cooperative environment. Such phenotypic changes often involve secretion of substances that can aid siblings and harm competitors (e.g., digestive enzymes, siderophores, and toxins; Miller and Bassler, 2001; Schuster et al., 2013). Notably, many bacterial pathogens use QS to initiate attack on a host only when they have amassed in a sufficient population number to overwhelm the host response. The link between pathogenesis and QS has attracted considerable recent interest to this communication network as a potential anti-infective target (Allen et al., 2014; Bjarnsholt and Givskov, 2007; Clatworthy et al., 2007). In turn, many symbionts use QS to initiate mutually beneficial relationships with their hosts, perhaps most conspicuously that between legumes and nitrogen-fixing rhizobia (Sanchez-Contreras et al., 2007).

Among the proteobacteria, QS is mostly achieved through the biosynthesis and subsequent concentration sensing of *N*-acyl L-homoserine lactone (AHL) signals. Within a given species, each bacterium synthesizes the same AHL constitutively at a low level (via LuxI-type synthases). Most AHLs can freely diffuse into and out of the cell. If the bacteria accumulate in an enclosed environment, the AHL concentration increases until it reaches a threshold intracellular level sufficient for productive binding and activation of its target receptor protein (termed a LuxR-type protein), which then alters the transcription of QS-regulated genes (Fuqua et al., 2001; Miller and Bassler, 2001). A typical LuxR-type protein is LasR from the opportunistic pathogen *Pseudomonas aeruginosa*. When its cognate signal AHL (*N*-(3-oxo)-dodecanoyl L-homoserine lactone, OdDHL, Figure 1) is present at a quorate concentration, LasR binds this signal and is stabilized by it in an active, dimerized form that recognizes certain promoters and recruits transcriptional machinery to induce QS gene expression (Sappington et al., 2011).

Because QS is dependent on the exchange of chemical signals, there is significant interest in the development of chemical probes that can prevent QS signal-receptor binding and alter QS outcomes. Indeed, the ability to modulate QS with non-native molecules has tremendous implications for artificially disrupting or promoting both pathogenic and mutualistic behavior (Galloway et al., 2011, 2012; Geske et al., 2008a). The spatial and temporal control afforded by chemical probes can enable a deeper understanding of important microbial phenotypes and possibly have direct therapeutic potential (Bjarnsholt and Givskov, 2007; Clatworthy et al., 2007; Praneenararat et al., 2012). As therapeutics, QS inhibitors have a prospective advantage over traditional antibiotic therapies, because recent socio-microbiology studies suggest that resistance is likely to spread more slowly to QS inhibitors (that target virulence phenotypes) than to traditional antibiotics (that target growth; Gerdt and Blackwell, 2014; Mellbye and Schuster, 2011). As such, QS inhibition is emerging as an important "antivirulence" approach (Allen et al., 2014; Clatworthy et al., 2007).

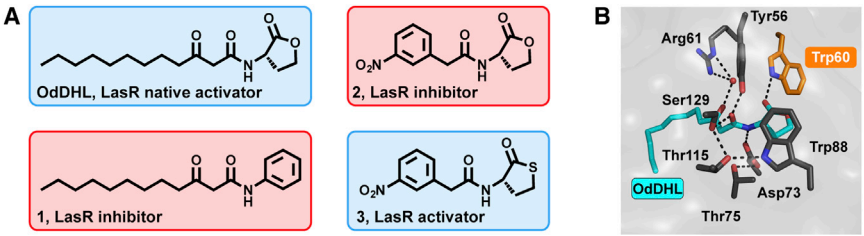

Figure 1. Impact of AHL Head Group on Ligand Activity in LasR

(A) Two pairs of ligands that share common acyl tails but have differing heads groups that govern LasR activation or inhibition.

(B) View of the OdDHL binding site in the [LasR:OdDHL]$_2$ X-ray crystal structure (Bottomley et al., 2007). Trp60 (highlighted in orange) hydrogen bonds to the lactone head group of OdDHL (cyan). Other residues that hydrogen bond with OdDHL or are part of a hydrogen-bonding network to OdDHL are displayed in gray. Hydrogen bonds are displayed as black dashed lines.

Some of the most well-studied chemical modulators of LasR are AHL analogs that have altered acyl tails, altered lactone heads, or both (Galloway et al., 2011; Hodgkinson et al., 2012; Mattmann and Blackwell, 2010). Generally, more attention has been given to variation in the acyl tail, but recently we and others have synthesized nonlactone versions of AHLs with the objective of both obtaining LasR ligands with enhanced hydrolytic stability and expanding our understanding of the structural features of the lactone head group that control ligand activity (Ishida et al., 2007; Jog et al., 2006; McInnis and Blackwell, 2011a, 2011b; Morkunas et al., 2012; Smith et al., 2003a, 2003b). These ligands certainly exhibit enhanced stabilities relative to lactone analogs—but more interestingly, some of our nonlactone ligands also have the opposite activity on LasR compared to their lactone analog. For example, aniline ligand **1** (Figure 1A) is an analog of the native activating ligand OdDHL, but it is a good inhibitor of LasR in reporter assays and in QS phenotypic assays (McInnis and Blackwell, 2011a; Morkunas et al., 2012). Other analogs of OdDHL with aniline head groups have also shown LasR inhibitory activity (Hodgkinson et al., 2012; McInnis and Blackwell, 2011a; Smith et al., 2003b). In addition, we observed that thiolactone **3** (Figure 1A) is a moderate activator of LasR, in contrast to its direct lactone analog **2**, which is instead a good inhibitor of LasR (Geske et al., 2007; McInnis and Blackwell, 2011b). These dramatic activity switches are seemingly caused by relatively subtle changes in ligand structure; however, the molecular bases for these flips in activity are unclear. In fact, there is virtually no information about the molecular mechanisms by which any non-native AHL analog modulates LuxR-type receptors (Ahumedo et al., 2014; Chen et al., 2011). Elucidating the causes of receptor activation versus inhibition by AHL analogs would not only improve our understanding of the molecular foundations of AHL-based QS, but would also augment our ability to design more potent molecular probes to modulate this signaling pathway. Toward this broad goal, we examined the origins of the activity flipping observed for the nonlactone LasR modulators **1** and **3** in the current study.

Herein, we report our investigations of interactions of LasR with nonlactone AHL analogs through the systematic mutagenesis of specific residues in the LasR native ligand binding site. We selected the residues for modification through study of the reported X-ray crystal structures of the LasR *N*-terminal ligand binding domain (residues 1–173, out of 239) bound to OdDHL (Bottomley et al., 2007; Zou and Nair, 2009), which permitted us to hypothesize determinants for LasR activation or inhibition by nonlactone AHLs. We subsequently tested these hypotheses via reporter gene assays using mutant LasRs. A similar mutagenesis approach was recently shown to be successful for studying the interactions of AHLs bearing non-native acyl groups with CviR, a LuxR-type receptor from *Chromobacterium violaceum* (Chen et al., 2011). Because the structures of analogs **1**–**3** closely approximate native AHLs, and analogs **1** and **2** act via competitive inhibition, we reasoned that they would also target the LasR ligand binding site; we therefore mutated the residues therein (Figure 1B). We found that mutation of Trp60, Tyr56, and Ser129 in LasR (Figure 1B) drastically flipped the activity of alternate head group ligands **1** and **3**. These observations led to the development of a model by which AHL analogs with different head groups exert opposite effects on LasR activity. As this model is further refined, we believe it will inform the design of next-generation QS modulators with heightened activities. The flipped-activity mutations identified in this work also have further implications—for the development of resistance to QS inhibitors and for use in synthetic biology. We end with a discussion of these two prospects.

RESULTS AND DISCUSSION

Importance of Trp60 in Governing LasR Activation and Inhibition by Nonlactone Ligands

Structural data for LuxR-type proteins bound to AHL ligands remains very limited (Churchill and Chen, 2011). However, each X-ray crystal structure of LasR and its homologs bound to an AHL reveals a hydrogen bond between the Trp60 (or homologous) side chain NH and the AHL lactone carbonyl (Bottomley et al., 2007; Chen et al., 2011; Lintz et al., 2011; Vannini et al., 2002; Zhang et al., 2002; Zou and Nair, 2009), and the Trp60 residue is highly conserved in LuxR-type proteins (Churchill and Chen, 2011). We hypothesized that the differential activity of alternative head-group ligands **1** and **3** toward LasR could be derived from different interactions of their nonlactone head groups with Trp60. To test this hypothesis, we mutated Trp60 in LasR to a phenylalanine residue, which has a smaller side chain that lacks a hydrogen-bond donor, but retains significant π character. We tested the activity of the mutant LasR using a β-galactosidase reporter in an *Escherichia coli* background (see Experimental Procedures). This W60F mutant was only moderately impaired at responding to OdDHL (Table S1 available online), but the activities of ligands **1** and **3** in the W60F mutant almost completely reverted back to the activities exhibited by their lactone counterparts (OdDHL and **2**, respectively) in both wild-type and W60F LasR (Table 1). Ligand **1**, which is an

Table 1. Activity of OdDHL and Ligands 1–3 in Wild-Type and W60F LasR

	Wild-Type				W60F			
Ligands	Activation (%)[a]	EC_{50} (nM)[b]	Inhibition (%)[a,c]	IC_{50} (nM)[b,c]	Activation (%)[a]	EC_{50} (nM)[b]	Inhibition (%)[a,c]	IC_{50} (nM)[b,c]
OdDHL	100	10	–	–	73	75	–	–
1	3[d]	–	54[d]	4,800	58	1,100	−17	–
2	0	–	80	510	1	–	81	3,700
3	82[d]	5,100	−13[d]	–	−13	–	98	550

[a]Ligands screened at 10 μM, arithmetic mean of biological triplicate is shown. No SEM exceeded 20%. Negative values for activation or inhibition mean the ligand is an inhibitor or activator, respectively, instead.
[b]Geometric mean of biological triplicate is shown. No arithmetic SEM of log-transformed data exceeded 0.14 (corresponding to an EC_{50} geometric standard error of ×/÷ 1.4; Limpert and Stahel, 2011).
[c]For inhibition, ligands were tested against EC_{50} of OdDHL (see Table S1).
[d]Data previously reported (McInnis and Blackwell, 2011a, 2011b).

inhibitor of wild-type LasR, reverts to being an activator in the W60F mutant like OdDHL. Conversely ligand **3**, which activates wild-type LasR, reverts to being an inhibitor in W60F, analogous to ligand **2**. We termed this interesting observation to be "Janus" behavior (after the two-faced Roman god of transitions), because the ligands transition between two vastly different activities depending on the identity of residue 60 in LasR. Although prior mutations to LasR homologs have demonstrated altered responses to AHLs (Chen et al., 2011; Collins et al., 2006), this observation is unique in that it involves only a single residue replacement, and this replacement flips both an inhibitor into an activator and an activator into an inhibitor. To verify that this Janus activity was not an artifact of the β-galactosidase reporter, we also tested ligands **1** and **3** in the W60F LasR mutant using a fluorescence reporter (Moore et al., 2014), and observed the same Janus profile. The striking reciprocal activities of these two ligands in wild-type LasR versus mutant LasR are apparent in Figures 2A and 2B.

Importance of Other LasR Residues in Governing Activation or Inhibition by Nonlactone Ligands

We were interested in ascertaining whether this Janus activity was unique to the Trp60 residue or if other hydrogen-bonding residues were similarly important at governing nonlactone ligand activity in LasR. We therefore mutated every residue in the LasR ligand-binding pocket that hydrogen bonds to OdDHL or is part of a hydrogen-bonding network with other residues that hydrogen bond with OdDHL (as shown in the $[LasR:OdDHL]_2$ structure; Figure 1B). The residues were mutated to amino acids that were of comparable size but lacked hydrogen-bonding ability (Y56F, R61M, D73L, T75V, W88F, T115V, and S129A). We constructed β-galactosidase reporters for each LasR mutant in *E. coli*, analogous to the W60F LasR mutant reporter above, and tested OdDHL and ligands **1**–**3** for mutant LasR activation and inhibition in each reporter. The Y56F and S129A mutants also showed Janus behavior (Figure 2C), but none of the other LasR mutants displayed such flipped activity relative to wild-type (Figure S1A). These non-Janus mutants were generally less strongly modulated by the ligands, presumably due to a missing polar interaction that leads to weaker ligand binding. Interestingly, unlike the W60F mutation that caused both ligand **1** and ligand **3** to flip activity from inhibitor to activator (and vice versa), the Y56F mutation only flipped the activity of ligand **1** from an inhibitor to an activator, and the S129A mutation only flipped the activity of ligand **3** from an activator to an inhibitor (Figure 2C). Ligand **3** remained an activator in the Y56F mutant, whereas ligand **1** displayed minimal activity in the S129A mutant. Both of the Tyr56 and Ser129 side chains engage in hydrogen bonds with the amide carbonyl of OdDHL in the $[LasR:OdDHL]_2$ structure (Figure 1B). Taken together, these LasR mutant data suggest that interactions of QS modulators **1**–**3** with these two amide-binding residues (Tyr56 and Ser129), along with Trp60, are important determinants for LasR activation and inhibition.

Trp60 has previously been hypothesized to be important for LasR:nonlactone ligand interactions. In 2006, Jog and colleagues proposed that altered interactions with Trp60 could explain why different stereoisomers of OdDHL analogs with cyclohexanol or cyclopentanol head groups activate LasR to different degrees (Jog et al., 2006); this study was performed prior to the report of the $[LasR:OdDHL]_2$ structure and was instead based upon analysis of the structure of TraR, a LuxR-type protein from *Agrobacterium tumefaciens*. In 2009, Zou and Nair modeled the synthetic triphenyl LasR inhibitor, TP-5, (Müh et al., 2006; shown in Figure S1B) into their X-ray crystal structure of LasR bound to an activating ligand (a related triphenyl derivative, TP-3), and suggested that a possible cause of the observed inhibitory activity for TP-5 (assuming this ligand targets the same ligand binding site) was the poor alignment of TP-5's chlorine atom with the Trp60 side chain NH for a halogen bond (Zou and Nair, 2009). We tested this hypothesis by examining the activity of TP-5 in the W60F LasR mutant. No Janus behavior was observed for TP-5 in this mutant—its LasR inhibitory activity was unchanged, and no LasR activation was observed (Figure S1A). These data reveal that mutation of Trp60 to Phe does not perturb interactions of TP-5 with LasR. Other mutations to Trp60 are necessary to gain further insights into the nature of Trp60 interactions with TP-5, if any. Nevertheless, these data for TP-5 indicate that this non-lactone inhibitor may make alternate contacts with LasR relative to ligands **1**–**3**.

Model for LasR Inhibition by Nonlactone QS Modulators

In view of the reporter strain data above, we developed a model to explain the activation and inhibition activity of these alternate head group ligands (**1** and **3**) in wild-type and mutant LasRs. Because wild-type LasR is inhibited by ligand **1** and the W60F mutation reverts **1** to an activator, we suspected that Trp60 interacts unfavorably with the aniline head of ligand **1**, which leads to

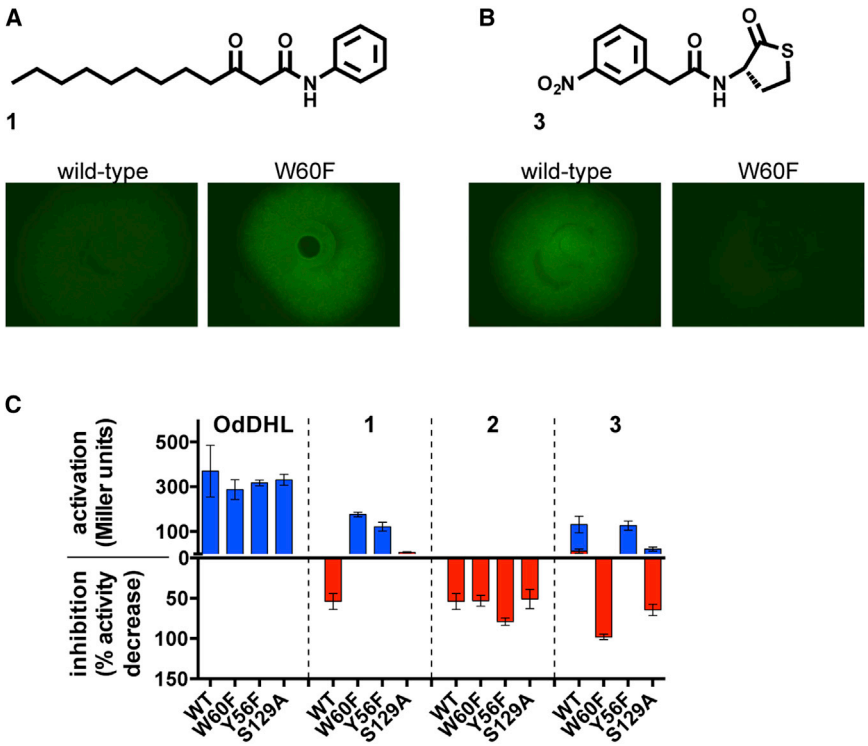

Figure 2. "Janus" Ligand-Protein Behavior

(A and B) Differential activation of green-fluorescent protein (GFP) expression by wild-type and W60F LasR in the presence of 10 μM ligands **1** and **3**.

(C) β-galactosidase reporter assays of wild-type LasR and three mutants with "Janus" behavior. Activation assays were performed by adding ligand at 10 μM, and activity is reporter as Miller units on the positive y-axis. Inhibition assays were performed by adding ligand at 10 μM and OdDHL at its EC_{50} value for that mutant (see Table S1), and activity is reported on the negative y-axis as the percent decrease in activity relative to only OdDHL being present. Error bars represent SEM of a biological triplicate.

an inactive LasR conformation. The replacement of tryptophan with the smaller phenylalanine residue relieves this unfavorable interaction, making the binding of ligand **1** compatible with the active conformation of LasR. To test this model at a more molecular level, Autodock (Morris et al., 2009) was used to computationally dock ligand **1** into the OdDHL-binding site of wild-type LasR and the (presumed) OdDHL-binding site of the W60F LasR mutant. We used the $[LasR:OdDHL]_2$ structure reported by Bottomley and colleagues for these computational studies (Bottomley et al., 2007; see Experimental Procedures). In agreement with our model, the lowest energy poses showed that the hydrogen *ortho* to the amide in the aniline head group of ligand **1** was consistently clashing with the NH of the Trp60 side chain (Figure 3A, orange arrow), whereas the W60F mutation enabled this *ortho* hydrogen to fit between two phenylalanine hydrogens with significantly longer atom-to-atom distances (Figure 3A). We of course are cautious to avoid firm structural conclusions based on docking results; nonetheless, the computational study suggests that Trp60 can indeed have unfavorable interactions with the aniline head of ligand **1** that are relieved by the W60F Janus mutation. This finding can be viewed as a "bump-hole" phenomenon (Bishop et al., 2000; Koh, 2002), where the aniline head provides a subtle "bump" that is sterically incompatible with Trp60 but is accommodated for by a "hole" formed by a tryptophan-to-phenylalanine mutation. Bump-hole approaches to modulating LuxR-type proteins with small molecules are yet to be reported, and this finding with LasR and ligand **1** provides impetus for exploration of this powerful chemical biology technique for the study of AHL-type QS.

Regarding ligands **2** and **3**, the wild-type activity data suggest that the thiolactone head group of ligand **3** enables it to bind wild-type LasR in a manner compatible with receptor activation, whereas the lactone ligand **2** binds LasR in a manner incompatible with receptor activation (Table 1). Because the W60F mutation abrogates this activation by ligand **3**, we suggest that the thiolactone is able to form a favorable hydrogen-bonding interaction that stabilizes Trp60 in LasR's active conformation, but the lactone of ligand **2** does not engage in this stabilizing interaction. Although natural bond order (NBO) analysis suggests that thiolactone carbonyls are not intrinsically better hydrogen bond acceptors than lactone carbonyls (see Table S2), docking of **3** into the LasR ligand binding site with Autodock (Morris et al., 2009) showed that the larger size of the thiolactone ring in **3** can position its carbonyl closer to the Trp60 side chain NH and also slightly further into the pocket (Figure 3B). Therefore, a model that matches our data and is molecularly reasonable posits that the thiolactone ligand **3** is better positioned to hydrogen bond with Trp60 and hold it in an orientation that stabilizes the active LasR conformation, whereas the smaller lactone of ligand **2** is improperly positioned for this active state stabilization. The W60F mutation causes both ligands to lose this hydrogen bond and therefore neither can position Phe60 in a conformation necessary for LasR activation. This model corroborates and serves to refine the earlier proposal by Jog and colleagues (vide supra), which invoked a prominent role for Trp60 in positioning the head groups of certain OdDHL analogs for differential LasR activation (Jog et al., 2006).

Finally, the observed importance of residues Tyr56 and Ser129—the side chains of which are known to hydrogen bond to the amide carbonyl of OdDHL (Figure 1B)—can be connected to this same model by considering how they position the ligands near Trp60. In the case of ligand **1**, Tyr56 may be essential in holding the ligand such that the aniline head group clashes with Trp60, allowing it to behave as a LasR inhibitor. In the case of ligand **3**, Ser129 may be essential in holding the ligand such that the thiolactone hydrogen bonds with Trp60, thereby engendering LasR activation.

It was still unclear how different orientations of Trp60 within the ligand-binding site, presumably caused by different ligand interactions, could regulate whether LasR was in an active or inactive

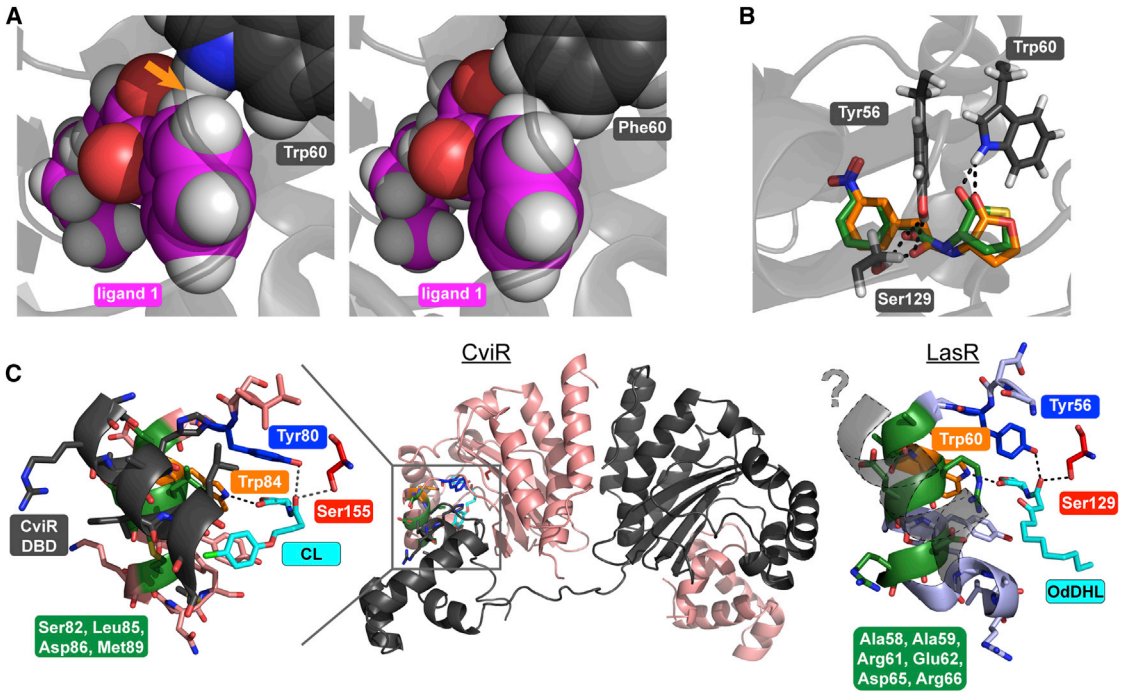

Figure 3. Model for Trp60 Governing LasR Activation versus Inhibition

(A) Images from automated docking of ligand **1** (magenta) into wild-type and W60F LasR, displaying steric clash between ligand **1** and Trp60 (see orange arrow) that is relieved in the W60F mutant.

(B) Image from automated docking of ligands **2** and **3** (orange and green, respectively) into wild-type LasR. Residues Tyr56 and Ser129 are shown hydrogen bonding to the ligand amide carbonyls, and Trp60 is shown hydrogen bonding to the lactone and thiolactone carbonyls with O–H distances of 2.2 Å and 1.8 Å, respectively.

(C) Images of X-ray crystal structures of $[CviR\text{-}CL]_2$ (Chen et al., 2011) and $[LasR\text{-}OdDHL]_2$ (Bottomley et al., 2007). Ligands (cyan) are shown interacting with Trp84 (CviR) and Trp60 (LasR) residues (orange), which are adjacent to residues (green) in an α helix that interacts with a binding partner (gray) in the inactive crossed-domain $[CviR\text{-}CL]_2$ structure (left inset). A hypothesized binding partner for LasR is displayed in transparent gray (right). Tyr56 and/or Ser129 homologous residues (blue and red, respectively) interact with the amide carbonyl to position the ligand lactone head near Trp60. Hydrogen bonds are displayed as dashed lines.

conformation. However, scrutiny of the reported X-ray structure of CviR bound to a non-native AHL ligand (CL) provided some insights (Chen et al., 2011). CL is a CviR antagonist, and the $[CviR:CL]_2$ homodimer structure revealed a crossed-domain conformation (Figure 3C), where the ligand-binding domain of each CviR monomer was bound to the DNA-binding domain of the other monomer. This conformation splayed the DNA-binding domains far apart from each other (relative to that observed in [LuxR-type protein:native AHL]$_2$ complexes), and the authors proposed that this structure is unable to bind DNA, belaying the mode of action of the antagonist CL. We observed that in this presumably inactive conformation, CviR engages in a protein-protein interaction adjacent to its Trp60 homologous residue (between residues Ser82, Leu85, Asp86, and Met89 adjacent to Trp84 and residues Thr246, His247, Ile249, and Val250 in the DNA-binding domain). We speculate that LasR could also form a homologous inactivating protein-protein interaction between residues near Trp60 (Ala58, Ala59, Arg61, Glu62, Asp65, Arg66) and the LasR DNA-binding domain or an alternative binding partner (as shown in Figure 3C). In support of this hypothesis, previous work on CviR showed that subtly different interactions between its ligands and Met89—a residue in the same inactivating protein-protein interface that interacts with the acyl tail of CviR-binding ligands—could alone drastically change whether the CviR dimer preferred the active or inactive conformation (Chen et al., 2011). We propose here that subtle positioning changes to Trp60 in LasR can similarly translate to the formation of the hypothesized inactivating protein-protein interaction. In total, our model posits that ligands with alternative head groups interact differently with Trp60 to alter Trp60's conformation enough to govern whether an adjacent inactivating protein-protein interaction is favorable. This model is consistent with the Janus behavior of the W60F, Y56F, and S129A mutants with ligands **1** and **3**, is logical on a molecular level, and relates well to the recently reported model for CviR inhibition by alternative tail ligands (Chen et al., 2011). Further studies are certainly necessary to test this model and are ongoing in our laboratory. Mutagenesis of the residues hypothesized to form inactivating protein-protein interactions near Trp60 is an important next step, as are structural studies of both wild-type LasR and W60F LasR bound to ligand **1**. Structures of full-length LasR, to augment the reported *N*-terminal ligand binding domain structures (Bottomley et al., 2007; Zou and Nair, 2009), would be particularly revealing with regard to probing interactions in the DNA binding domain.

Further Implications and Conclusions

The results reported herein yield a model to explain LasR activation and inhibition by AHL analogs with non-native head groups. However, they also afford two other important implications. First, the observation that a single amino acid mutation (W60F or Y56F) can make LasR immune to QS inhibitor **1**, as well as similar findings with other LuxR-type proteins (Chen et al., 2011; Collins et al., 2006), demonstrates that a likely mechanism of resistance to QS inhibitors is mutation of LuxR-type proteins. We find it particularly interesting that the W60F and Y56F LasR mutants became activated by an inhibitor, which would lead to a "signal-independent" mechanism of QS-inhibitor resistance (i.e., native OdDHL signal would not be required for QS activation of the mutant as long as the inhibitor-turned-activator is present). We have recently discussed the implications of such signal-independent QS-inhibitor resistance pathways (Gerdt and Blackwell, 2014). However, as we and others have shown, QS inhibitors should hold a decreased spread of resistance compared to traditional antibiotics due to the competition that arises after a resistant bacterium appears (Gerdt and Blackwell, 2014; Mellbye and Schuster, 2011; Schuster et al., 2013). Therefore, even though resistance can readily develop (via the LuxR-type receptor mutations examined here or other potential paths), it should not spread easily, and the application of QS inhibitors as resistance-robust microbial control agents still holds significant promise.

The second interesting implication of the three LasR mutants (W60F, Y56F, and S129A) is their potential use in bioengineering applications. The emerging field of synthetic biology requires the precise control of gene expression (Khalil and Collins, 2010). For complex applications, this requires several orthogonal gene regulatory elements. Some of the most common inducible gene-expression systems suffer from crosstalk and are based on metabolic regulation, which can influence metabolism as an undesired side effect (Lee et al., 2007). Thus AHL-based QS systems have found significant recent utility in expanding the toolbox of orthogonal inducible gene-expression elements (Collins et al., 2006; Cox et al., 2007; Li et al., 2011; Tamsir et al., 2011). A limitation of natural AHLs is their relative hydrolytic instability (Byers et al., 2002), which is alleviated substantially by replacing their lactone head groups with stable non-lactone variants (such as **1** and **3**; Hodgkinson et al., 2012; Ishida et al., 2007; Jog et al., 2006; McInnis and Blackwell, 2011a, 2011b; Morkunas et al., 2012; Smith et al., 2003a, 2003b). The W60F, Y56F, and S129A LasR mutants reported herein, which respond in opposite ways to the same nonlactone ligands, enable methods of complex regulated gene expression that could provide for interesting experiments with mixed bacterial populations. For example, a gene in one organism could be induced by addition of ligand **1**, and then addition of ligand **3** would both afford induction of a gene in a second organism and shut off the first. This mixed-population "pulse-chase" technique would have the benefit of not requiring the removal of the initial signal molecule from the medium, and concomitantly uses ligands that should not influence metabolism and are more hydrolytically stable than native AHLs. Many other experimental scenarios are conceivable, as well.

In conclusion, we have delineated insights into the mechanisms by which nonlactone ligands influence activation and inhibition of LasR—a QS receptor that regulates the virulence of the prevalent opportunistic pathogen *P. aeruginosa*. Our site-directed mutagenesis and structural analyses provide empirical evidence that aniline and thiolactone ligand head groups interact differently with Trp60 relative to lactone head groups, and that this differential interaction is sufficient to govern complete flips between marked activation and inhibition of LasR. Based on the $[CviR:CL]_2$ cocrystal structure (Chen et al., 2011), we proposed a model by which different interactions with Trp60 could translate to an inactive conformation of LasR. The reported data and model are significant because the field has practically no information about the molecular mechanisms by which synthetic activators and inhibitors interact with LasR. As this model is further explored, we believe that it should provide insights for the design of new synthetic LasR modulators with improved efficacies. For example, we could intentionally design ligands that will displace Trp60 more drastically. Alternatively, if we discover that the hypothesized inactivating protein-protein interaction is in fact operative in LasR, we can attempt to rationally stabilize or destabilize it to control LasR activity. Lastly, looking beyond the mechanistic outcomes of this study, the exciting discovery of Janus behavior between different LasR mutants both demonstrates a mechanism by which signal-independent resistance can develop to QS inhibition and holds implications for engineered gene regulation.

SIGNIFICANCE

Quorum sensing (QS) is a mechanism that hundreds of bacterial species use to sense their population density by detecting the concentration of secreted signal molecules. QS regulates many virulence phenotypes in pathogens such as *Pseudomonas aeruginosa* and beneficial phenotypes in mutualistic symbionts. Therefore, the development of potent QS modulating small molecules could have significant utility for use as experimental tools and possibly as therapeutics. Although numerous synthetic activators and inhibitors of *N*-acyl L-homoserine lactone (AHL)-type QS have been reported, their molecular basis of activation and inhibition is largely unknown. Subtly different molecules can have opposite activities, and the difficulty of structurally characterizing QS receptor proteins like LasR from *P. aeruginosa* makes this problem challenging. We recently identified a set of nonlactone AHL analogs with enhanced hydrolytic stability and strong agonistic and antagonistic activity in LasR. In the current study, we sought to investigate how differences in the lactone heads of QS modulators can drastically change their activity in LasR and its homologs. We undertook mutational analysis of LasR coupled with reporter gene activity assays with four different ligands and found that Trp60, Tyr56, and Ser129 are crucial in determining whether a nonlactone QS modulator is an activator or an inhibitor of LasR. Using these data, we developed a model to explain the mechanisms by which the ligands can activate or inactivate LasR. This model will help in the design of improved molecular tools to control QS and the virulence phenotypes it regulates. Additionally, our finding of a set of ligands and mutant LasRs that present "Janus" activity (i.e., individual ligands that are "two-faced" by inhibiting

wild-type LasR but activating a mutant, and vice-versa) can find significant utility for differentially controlling gene expression in synthetic biology applications.

EXPERIMENTAL PROCEDURES

Compound Handling and Reagents

Stock solutions of synthetic compounds (10 mM) were prepared in DMSO and stored at room temperature in sealed vials. OdDHL, **1**, **2**, and **3** were synthesized as previously reported (Geske et al., 2008b; McInnis and Blackwell, 2011a, b). The synthesis and characterization of the TP-5 ligand is reported in the Supplemental Experimental Procedures. Solvent-resistant polypropylene (Corning Costar cat. no. 3790) and clear polystyrene (Corning Costar cat. no. 3997) 96-well microtiter plates were used as appropriate.

Bacterial Strains, Media, and Growth Conditions

The bacterial strains used in this study were *E. coli* DH5α [F^- φ80d*lacZ*Δ*M15* Δ(*lacZYA-argF*)*U169 deoR recA1 endA1 hsdR17*(r_K^- m_K^+) *phoA supE44* λ^- *thi-1 gyrA96 relA1*] and *E. coli* K-12 derivative JLD271 (Lindsay and Ahmer, 2005). See the Supplemental Experimental Procedures for list of strains and plasmids. *E. coli* was cultured at 37°C in Luria-Bertani (LB) medium and on LB plates with 1.5% agar. For selection and maintenance of plasmids, gentamicin, ampicillin, and kanamycin were used at 15 μg/ml, 100 μg/ml, and 50 μg/ml, respectively.

Construction of Mutant LasR Reporter Strains

Site-directed mutagenesis was carried out on the LasR-expressing plasmid pJN105L (Lee et al., 2006) by overlap extension PCR (Heckman and Pease, 2007; see the Supplemental Experimental Procedures for PCR primers). The mutagenized *lasR* genes were digested with *EcoRI* and *XbaI* and cloned into *EcoRI*/*XbaI*-cut pJN105L (Lee et al., 2006). The mutant pJN105L variants were sequenced to verify mutagenesis and transformed via electroporation into the *E. coli* DH5α/pSC11 (Chugani et al., 2001) reporter strain and selected on LB + gentamicin + ampicillin plates.

β-Galactosidase Reporter Gene Assays

All assays were conducted as previously reported (McInnis and Blackwell, 2011a, b) for the *E. coli* wild-type LasR strain DH5α/pJN105L + pSC11 (Lee et al., 2006). Absorbance measurements were obtained using a Biotek Synergy monochromator plate reader running Gen5 v1.05 software. A 600 nm filter was used for reading bacterial cell density. Filters of 420 nm and 550 nm were used for Miller-type absorbance assays. OdDHL EC_{50} values were calculated for all LasR mutant strains (Table S1) by reported dose-response methods (McInnis and Blackwell, 2011b). Synthetic ligands were tested for LasR activation at 10 μM in each strain. Similarly, ligands were tested for LasR inhibition at 10 μM against OdDHL at its EC_{50} value (Table S1) for the mutant LasR strain.

Fluorescence Microscopy

To prepare the fluorescent reporter strains, the same pJN105L-derived mutant plasmids were transformed into *E. coli* JLD271/pPROBE-KL (Moore et al., 2014) via electroporation and selection on LB + gentamicin + kanamycin. Microscopy was performed with a Zeiss AX10 Imager.M2 epifluorescent microscope with a HXP 120 C Lamp using the 2.5×/0.12 FLUAR objective in conjunction with an AxioCam MR monochrome camera controlled by AxioVision (Rel 4.8.2) software (Carl Zeiss MicroImaging). GFP filters was used. Microscopy was performed directly through an LB agar plate containing 10 μM **1** or **3** and 0.4% arabinose after inoculation with approximately 10^5 colony-forming units of the *E. coli* fluorescent reporter strains and incubation at 37°C for 9 hr.

Ligand Docking

All four ligands discussed in this work were computationally docked into wild-type LasR and W60F LasR structures using AutoDock v.4.2 (Morris et al., 2009). The LasR structure was generated from the $[LasR:OdDHL]_2$ structure (Protein Data Bank [PDB] ID 2UV0; Bottomley et al., 2007). Using SYBYL-X 2.1.1 (Certara, L.P.), the native ligand and all water molecules were removed. To generate the structure of the W60F mutant, Trp60 was replaced with Phe. For both structures, all hydrogen atoms were added. The four ligands (OdDHL and **1**–**3**) were built and geometry optimized in Sybyl using the Powell method with 0.05 kcal/(mol*Å) gradients and 100 maximum iterations, using Simplex initial optimization, Tripos force field, and Gasteiger-Huckel charges. Docking dimensions were set in ADT Autodock Tools and were centered on the binding pocket with a size that included the entire pocket. Autodock was then used to dock all four ligands with 30 trials, population size of 100, random starting position and conformation, translation step range of 2.0 Å, rotation step ranges of 50°, elitism of 1, mutation rate of 0.02, crossover rate of 0.8, local search rate of 0.06, and 1,000,000 maximum energy evaluations. As a test of the docking quality, the docking of OdDHL was compared to its position in the original X-ray crystal structure (PDB ID 2UV0), and it was observed to overlap extremely well (Figure S2A). The lowest energy poses that bound in the pocket similarly to OdDHL are displayed in Figures 3A and 3B and are representative of other low-energy poses. Ensembles of all the docking poses are shown in Figure S2. All structural images were generated in PyMol 1.3 (Schrödinger).

Statistical Analysis

The error bars in all plots represent SEM from a biological triplicate.

SUPPLEMENTAL INFORMATION

Supplemental Information includes Supplemental Experimental Procedures, two figures, and two tables and can be found with this article online at http://dx.doi.org/10.1016/j.chembiol.2014.08.008.

AUTHOR CONTRIBUTIONS

J.P.G., C.E.M., and H.E.B. designed the research and wrote the paper; J.P.G. and C.E.M. analyzed data; J.P.G. prepared mutant LasR strains, performed fluorescence assays, and docking and NBO analysis; C.E.M. synthesized OdDHL and ligands **1–3,** and performed β-galactosidase assays; T.L.S. performed β-galactosidase assays; and F.M.R. synthesized and characterized ligand TP-5.

ACKNOWLEDGMENTS

Financial support was provided by the NIH (GM109403), the National Science Foundation (NSF; CHE-1213526), and the Burroughs Wellcome Foundation. J.P.G. and C.E.M. were each supported in part by the Department of Defense Air Force Office of Scientific Research through National Defense Science & Engineering Graduate fellowships (32 CFR 168a). J.P.G. was also supported in part by the NIH through the UW-Madison Chemistry-Biology Interface Training Grant (NIGMS T32 GM008505). Support for the NMR and MS facilities in the UW-Madison Chemistry Department was provided by the NSF (CHE-1048642, CHE-9974839). The funders had no role in study design, data collection and analysis, decision to publish, or preparation of the manuscript. We thank Professor Edward Ruby for microscope use, Dr. Kenneth Satyshur for assistance with computational analyses, and Robert Newberry for aid in NBO analysis.

Received: June 20, 2014
Revised: August 5, 2014
Accepted: August 18, 2014
Published: September 18, 2014

REFERENCES

Ahumedo, M., Drosos, J.C., and Vivas-Reyes, R. (2014). Application of molecular docking and ONIOM methods for the description of interactions between anti-quorum sensing active (AHL) analogues and the *Pseudomonas aeruginosa* LasR binding site. Mol. Biosyst. *10*, 1162–1171.

Allen, R.C., Popat, R., Diggle, S.P., and Brown, S.P. (2014). Targeting virulence: can we make evolution-proof drugs? Nat. Rev. Microbiol. *12*, 300–308.

Bishop, A., Buzko, O., Heyeck-Dumas, S., Jung, I., Kraybill, B., Liu, Y., Shah, K., Ulrich, S., Witucki, L., Yang, F., et al. (2000). Unnatural ligands for

engineered proteins: new tools for chemical genetics. Annu. Rev. Biophys. Biomol. Struct. *29*, 577–606.

Bjarnsholt, T., and Givskov, M. (2007). Quorum-sensing blockade as a strategy for enhancing host defences against bacterial pathogens. Philos. Trans. R. Soc. Lond. B Biol. Sci. *362*, 1213–1222.

Bottomley, M.J., Muraglia, E., Bazzo, R., and Carfi, A. (2007). Molecular insights into quorum sensing in the human pathogen *Pseudomonas aeruginosa* from the structure of the virulence regulator LasR bound to its autoinducer. J. Biol. Chem. *282*, 13592–13600.

Byers, J.T., Lucas, C., Salmond, G.P., and Welch, M. (2002). Nonenzymatic turnover of an *Erwinia carotovora* quorum-sensing signaling molecule. J. Bacteriol. *184*, 1163–1171.

Chen, G., Swem, L.R., Swem, D.L., Stauff, D.L., O'Loughlin, C.T., Jeffrey, P.D., Bassler, B.L., and Hughson, F.M. (2011). A strategy for antagonizing quorum sensing. Mol. Cell *42*, 199–209.

Chugani, S.A., Whiteley, M., Lee, K.M., D'Argenio, D., Manoil, C., and Greenberg, E.P. (2001). QscR, a modulator of quorum-sensing signal synthesis and virulence in *Pseudomonas aeruginosa*. Proc. Natl. Acad. Sci. USA *98*, 2752–2757.

Churchill, M.E.A., and Chen, L. (2011). Structural basis of acyl-homoserine lactone-dependent signaling. Chem. Rev. *111*, 68–85.

Clatworthy, A.E., Pierson, E., and Hung, D.T. (2007). Targeting virulence: a new paradigm for antimicrobial therapy. Nat. Chem. Biol. *3*, 541–548.

Collins, C.H., Leadbetter, J.R., and Arnold, F.H. (2006). Dual selection enhances the signaling specificity of a variant of the quorum-sensing transcriptional activator LuxR. Nat. Biotechnol. *24*, 708–712.

Cox, R.S., 3rd, Surette, M.G., and Elowitz, M.B. (2007). Programming gene expression with combinatorial promoters. Mol. Syst. Biol. *3*, 145.

Fuqua, C., Parsek, M.R., and Greenberg, E.P. (2001). Regulation of gene expression by cell-to-cell communication: acyl-homoserine lactone quorum sensing. Annu. Rev. Genet. *35*, 439–468.

Galloway, W.R.J.D., Hodgkinson, J.T., Bowden, S.D., Welch, M., and Spring, D.R. (2011). Quorum sensing in Gram-negative bacteria: small-molecule modulation of AHL and AI-2 quorum sensing pathways. Chem. Rev. *111*, 28–67.

Galloway, W.R.J.D., Hodgkinson, J.T., Bowden, S., Welch, M., and Spring, D.R. (2012). Applications of small molecule activators and inhibitors of quorum sensing in Gram-negative bacteria. Trends Microbiol. *20*, 449–458.

Gerdt, J.P., and Blackwell, H.E. (2014). Competition studies confirm two major barriers that can preclude the spread of resistance to quorum-sensing inhibitors in bacteria. ACS Chem. Biol. Published online August 8, 2014. http://dx.doi.org/10.1021/cb5004288.

Geske, G.D., O'Neill, J.C., Miller, D.M., Mattmann, M.E., and Blackwell, H.E. (2007). Modulation of bacterial quorum sensing with synthetic ligands: systematic evaluation of *N*-acylated homoserine lactones in multiple species and new insights into their mechanisms of action. J. Am. Chem. Soc. *129*, 13613–13625.

Geske, G.D., O'Neill, J.C., and Blackwell, H.E. (2008a). Expanding dialogues: from natural autoinducers to non-natural analogues that modulate quorum sensing in Gram-negative bacteria. Chem. Soc. Rev. *37*, 1432–1447.

Geske, G.D., O'Neill, J.C., Miller, D.M., Wezeman, R.J., Mattmann, M.E., Lin, Q., and Blackwell, H.E. (2008b). Comparative analyses of *N*-acylated homoserine lactones reveal unique structural features that dictate their ability to activate or inhibit quorum sensing. ChemBioChem *9*, 389–400.

Heckman, K.L., and Pease, L.R. (2007). Gene splicing and mutagenesis by PCR-driven overlap extension. Nat. Protoc. *2*, 924–932.

Hodgkinson, J.T., Galloway, W.R.J.D., Wright, M., Mati, I.K., Nicholson, R.L., Welch, M., and Spring, D.R. (2012). Design, synthesis and biological evaluation of non-natural modulators of quorum sensing in *Pseudomonas aeruginosa*. Org. Biomol. Chem. *10*, 6032–6044.

Ishida, T., Ikeda, T., Takiguchi, N., Kuroda, A., Ohtake, H., and Kato, J. (2007). Inhibition of quorum sensing in *Pseudomonas aeruginosa* by *N*-acyl cyclopentylamides. Appl. Environ. Microbiol. *73*, 3183–3188.

Jog, G.J., Igarashi, J., and Suga, H. (2006). Stereoisomers of *P. aeruginosa* autoinducer analog to probe the regulator binding site. Chem. Biol. *13*, 123–128.

Khalil, A.S., and Collins, J.J. (2010). Synthetic biology: applications come of age. Nat. Rev. Genet. *11*, 367–379.

Koh, J.T. (2002). Engineering selectivity and discrimination into ligand-receptor interfaces. Chem. Biol. *9*, 17–23.

Lee, J.-H., Lequette, Y., and Greenberg, E.P. (2006). Activity of purified QscR, a *Pseudomonas aeruginosa* orphan quorum-sensing transcription factor. Mol. Microbiol. *59*, 602–609.

Lee, S.K., Chou, H.H., Pfleger, B.F., Newman, J.D., Yoshikuni, Y., and Keasling, J.D. (2007). Directed evolution of AraC for improved compatibility of arabinose- and lactose-inducible promoters. Appl. Environ. Microbiol. *73*, 5711–5715.

Li, Z., Rosenbaum, M.A., Venkataraman, A., Tam, T.K., Katz, E., and Angenent, L.T. (2011). Bacteria-based AND logic gate: a decision-making and self-powered biosensor. Chem. Commun. (Camb.) *47*, 3060–3062.

Limpert, E., and Stahel, W.A. (2011). Problems with using the normal distribution—and ways to improve quality and efficiency of data analysis. PLoS ONE *6*, e21403.

Lindsay, A., and Ahmer, B.M.M. (2005). Effect of *sdiA* on biosensors of *N*-acylhomoserine lactones. J. Bacteriol. *187*, 5054–5058.

Lintz, M.J., Oinuma, K., Wysoczynski, C.L., Greenberg, E.P., and Churchill, M.E.A. (2011). Crystal structure of QscR, a *Pseudomonas aeruginosa* quorum sensing signal receptor. Proc. Natl. Acad. Sci. USA *108*, 15763–15768.

Mattmann, M.E., and Blackwell, H.E. (2010). Small molecules that modulate quorum sensing and control virulence in *Pseudomonas aeruginosa*. J. Org. Chem. *75*, 6737–6746.

McInnis, C.E., and Blackwell, H.E. (2011a). Design, synthesis, and biological evaluation of abiotic, non-lactone modulators of LuxR-type quorum sensing. Bioorg. Med. Chem. *19*, 4812–4819.

McInnis, C.E., and Blackwell, H.E. (2011b). Thiolactone modulators of quorum sensing revealed through library design and screening. Bioorg. Med. Chem. *19*, 4820–4828.

Mellbye, B., and Schuster, M. (2011). The sociomicrobiology of antivirulence drug resistance: a proof of concept. mBio *2*, e00131–11.

Miller, M.B., and Bassler, B.L. (2001). Quorum sensing in bacteria. Annu. Rev. Microbiol. *55*, 165–199.

Moore, J.D., Gerdt, J.P., Eibergen, N.R., and Blackwell, H.E. (2014). Active efflux influences the potency of quorum sensing inhibitors in *Pseudomonas aeruginosa*. ChemBioChem *15*, 435–442.

Morkunas, B., Galloway, W.R.J.D., Wright, M., Ibbeson, B.M., Hodgkinson, J.T., O'Connell, K.M.G., Bartolucci, N., Della Valle, M., Welch, M., and Spring, D.R. (2012). Inhibition of the production of the *Pseudomonas aeruginosa* virulence factor pyocyanin in wild-type cells by quorum sensing autoinducer-mimics. Org. Biomol. Chem. *10*, 8452–8464.

Morris, G.M., Huey, R., Lindstrom, W., Sanner, M.F., Belew, R.K., Goodsell, D.S., and Olson, A.J. (2009). AutoDock4 and AutoDockTools4: Automated docking with selective receptor flexibility. J. Comput. Chem. *30*, 2785–2791.

Müh, U., Schuster, M., Heim, R., Singh, A., Olson, E.R., and Greenberg, E.P. (2006). Novel *Pseudomonas aeruginosa* quorum-sensing inhibitors identified in an ultra-high-throughput screen. Antimicrob. Agents Chemother. *50*, 3674–3679.

Praneenararat, T., Palmer, A.G., and Blackwell, H.E. (2012). Chemical methods to interrogate bacterial quorum sensing pathways. Org. Biomol. Chem. *10*, 8189–8199.

Sanchez-Contreras, M., Bauer, W.D., Gao, M., Robinson, J.B., and Allan Downie, J. (2007). Quorum-sensing regulation in rhizobia and its role in symbiotic interactions with legumes. Philos. Trans. R. Soc. Lond. B Biol. Sci. *362*, 1149–1163.

Sappington, K.J., Dandekar, A.A., Oinuma, K.-I., and Greenberg, E.P. (2011). Reversible signal binding by the Pseudomonas aeruginosa quorum-sensing signal receptor LasR. mBio *2*, e00011–11.

Schuster, M., Sexton, D.J., Diggle, S.P., and Greenberg, E.P. (2013). Acyl-homoserine lactone quorum sensing: from evolution to application. Annu. Rev. Microbiol. *67*, 43–63.

Smith, K.M., Bu, Y., and Suga, H. (2003a). Induction and inhibition of *Pseudomonas aeruginosa* quorum sensing by synthetic autoinducer analogs. Chem. Biol. *10*, 81–89.

Smith, K.M., Bu, Y., and Suga, H. (2003b). Library screening for synthetic agonists and antagonists of a *Pseudomonas aeruginosa* autoinducer. Chem. Biol. *10*, 563–571.

Tamsir, A., Tabor, J.J., and Voigt, C.A. (2011). Robust multicellular computing using genetically encoded NOR gates and chemical 'wires'. Nature *469*, 212–215.

Vannini, A., Volpari, C., Gargioli, C., Muraglia, E., Cortese, R., De Francesco, R., Neddermann, P., and Marco, S.D. (2002). The crystal structure of the quorum sensing protein TraR bound to its autoinducer and target DNA. EMBO J. *21*, 4393–4401.

Zhang, R.G., Pappas, K.M., Brace, J.L., Miller, P.C., Oulmassov, T., Molyneaux, J.M., Anderson, J.C., Bashkin, J.K., Winans, S.C., and Joachimiak, A. (2002). Structure of a bacterial quorum-sensing transcription factor complexed with pheromone and DNA. Nature *417*, 971–974.

Zou, Y., and Nair, S.K. (2009). Molecular basis for the recognition of structurally distinct autoinducer mimics by the *Pseudomonas aeruginosa* LasR quorum-sensing signaling receptor. Chem. Biol. *16*, 961–970.